Contribution from the Department of Chemistry,
University of Arizona, Tucson, Arizona 85721

Excited-State Ordering and Solvatochromic Emission in (Pyridine)- and (Poly(pyridine))chromium(III) Complexes

Abdulatif M. Ghaith, Leslie S. Forster,* and John V. Rund

Received September 9, 1986

The 77 K emission spectra and excited-state decays of *trans*-$Cr(py)_4F_2^+$, *cis*-$Cr(phen)_2F_2^+$, *cis*-$Cr(bpy)_2Cl_2^+$, *trans*-$Cr(py)_4FBr^+$, and $Cr(bpy)_3^{3+}$ have been recorded in hydroxylic and nonhydroxylic glasses. The character of the emission depends upon the relative dispositions of the ^2E level and one of the $^2T_1$ components. The energies of these levels are determined by intramolecular and environmental factors, and solvent-induced level inversion occurs in *cis*-$Cr(phen)_2F_2^+$. Multiple solvate effects are most important when the two excited levels are proximate. The emission spectral changes in DMF/H_2O solutions suggest that the solvent cavity size depends on the composition. Evidence to support the assignment of a negative π-donation angular overlap model parameter to pyridine is presented.

Introduction

With very few exceptions, Cr(III) complexes luminesce at low temperatures, and the photophysics of more than 200 complexes has been studied. The emission is usually due to the $^2E \rightarrow {}^4A_2$ transition, and neither the lifetime nor the narrow emission spectrum is sensitive to solvent in rigid media.[2] In nearly cubic fields $^2T_1$ is some 500 cm^{-1} above ^2E.[3] When the symmetry is reduced by a tetragonal field, $^2T_1$ is split and a number of complexes have been identified in which the quadrate field is large enough to depress one of the $^2T_1$ components, $^2E^Q$, below ^2E.[4] The resultant $^2E^Q \rightarrow {}^4A_2$ spectrum is broad with a solvent-dependent position.[2b] The 77 K emissions in *cis*-$Cr(NH_3)_4(OH)_2^+$ and *cis*-$Cr(en)_2(OH)_2^+$ are narrow in hydroxylic solvents but broadened and shifted to longer wavelengths in DMF/H_2O. This behavior was attributed to the near coincidence of the ^2E and $^2E^Q$ energies.[2b] The differential solvent effect on the two levels then leads to $^2E \rightarrow {}^4A_2$ emission in hydroxylic solvents and to a $^2E^Q \rightarrow {}^4A_2$ spectrum in DMF/H_2O. The time-resolved emission spectrum of *cis*-$Cr(NH_3)_4(OH)_2^+$ in DMF/H_2O varies with the delay,[2b] indicating emission from several solvates in this medium.

Prerequisite to the study of the effect of temperature and solvent relaxation on the photophysical properties of Cr(III) complexes is an understanding of the solvate behavior in rigid media. Among the (pyridine)- and (poly(pyridine))chromium(III) complexes are species with varying ^2E–$^2E^Q$ dispositions. We now describe the effect of environment on the low-temperature emission spectra and excited-state relaxation rates from a group of these complexes with special emphasis on those species in which the ^2E and $^2E^Q$ levels are proximate.

Experimental Section

cis-$[Cr(phen)_2F_2](ClO_4)$[1] and *trans*-$[Cr(py)_4F_2](NO_3)$ were synthesized by literature methods.[5] *cis*-$[Cr(bpy)_2Cl_2]Cl\cdot 2H_2O$, *cis*-$[Cr(bpy)_2(H_2O)(OH)](ClO_4)_2$, and *cis*-$[Cr(bpy)_2F_2](ClO_4)$ were generously provided by J. Josephsen. *trans*-$[Cr(py)_4FBr](ClO_4)$, *trans*-$[Cr(py)_4Cl_2](ClO_4)\cdot H_2O$, *trans*-$[Cr(py)_4Br_2](ClO_4)$, and *trans*-$[Cr(py)_4(H_2O)_2](ClO_4)_3$ were gifts from J. Glerup. Ethylene glycol, glycerol, methyltetrahydrofuran, and DMF were reagent grade and, with the exception of DMF, used without further purification. When required, DMF was dried over CaO at reduced N_2 pressure.

Time-resolved spectra and lifetimes were determined with an N_2 laser (337 nm), or by a N_2 laser-pumped fluorescein dye laser (545 nm), as described elsewhere.[2b] The aperture time in the boxcar integrator was 0.5 μs.

The lifetimes were calculated by fitting the decays in the interval $I(0)$–$0.10I(0)$ to a single exponential function. Nonexponentiality was characterized by comparison of the average lifetimes over the first and last 25% of this interval, i.e., $\bar{\tau}_f/\bar{\tau}_i$. When this ratio is less than 1.05, the time-resolved emission spectra are invariant to delay time and the decay is described as exponential.

Results

***cis*-$Cr(phen)_2F_2^+$.** The time-resolved spectra of *cis*-$Cr(phen)_2F_2^+$ in several rigid glassy solvents at 77 K are compared to the emission of pure solid *cis*-$[Cr(phen)_2F_2](ClO_4)$ in Figures 1 and 2. The spectrum in EGW is narrow while that in pure DMF is broad and shifted to longer wavelengths. The difference of the *cis*-$Cr(phen)_2F_2^+$ emission energy in the crystalline solid and DMF is noteworthy. This broad spectrum moves progressively to the blue as the water content is increased. At high water levels, the emission in DMF/H_2O resembles the EGW spectrum. The EGW emission spectrum is the same under 337- and 545-nm excitation.

The spectrum in EGW is only slightly dependent on delay time (Figures 1 and 2) while in dry DMF the spectrum sharpens and is shifted to the blue with increasing delay. When a solution of *cis*-$Cr(phen)_2F_2^+$ in dry DMF is frozen, the character of the resultant solid depends upon the rate of cooling. An opaque mass is usually produced, but if the cuvette diameter is sufficiently small, plunging the sample into liquid N_2 yields a glass. If this solution is heated to 158 K, an opaque mass forms quickly and the emission spectrum is shifted to the blue. Presumably the host is now a microcrystalline solid. A small amount of water in DMF is always sufficient to produce a good glass by rapid cooling in liquid N_2. At each delay, the shape of the spectrum in the opaque solid closely resembles that in the dry glass, but the position is blue-shifted relative to the glass.

When the emission is monitored at 720 nm the excited state decay in EGW is fairly exponential with $t \simeq 1500$ μs. As the monitoring wavelength is increased, the decay becomes slightly faster (Table I). In DMF/H_2O mixtures the decays become faster and more nonexponential at longer wavelengths.

The emission spectrum in glassy 2-ME is very dependent on delay time (Figure 3). At 25 μs the emission is broad and similar to that in DMF/H_2O at $X_{H_2O} = 0.65$. At long delay the emission is much sharper and is hardly distinguishable from the EGW spectrum. The spectral behavior is reflected in the wavelength variation of the decay times (Table I). The 730-nm decay is fairly exponential with $\tau = 1200$ μs, nearly the same magnitude that prevails in EGW and DMF/H_2O at the same wavelength. The decay becomes faster and less exponential as the monitoring wavelength is increased.

The emission in pure solid *cis*-$[Cr(phen)_2F_2](ClO_4)$ is invariant to delay time and is found at the longest wavelengths.

(1) Abbreviations: py, pyridine; bpy, 2,2′-bipyridine; phen, 1,10-phenanthroline; en, 1,2-ethanediamine; DMF, dimethylformamide; EGW, ethylene glycol/water, 2:1 (v/v); 2-ME, 2-methoxyethanol; MTHF, methyltetrahydrofuran.

(2) (a) Forster, L. S. *Adv. Chem. Ser.* **1976**, *No. 150*, 172. (b) Fucaloro, A. F.; Forster, L. S.; Kirk, A. D.; Glover, S. G. *Inorg. Chem.* **1985**, *24*, 4242.
(3) Flint, C. D.; Mathews, A. P. *J. Chem. Soc., Faraday Trans. 2* **1976**, *72*, 579.
(4) Flint, C. E.; Mathews, A. P. *Inorg. Chem.* **1975**, *14*, 1008; *J. Chem. Soc., Faraday Trans. 2* **1974**, *70*, 1307.
(5) Glerup, J.; Josephsen, J.; Michelsen, K.; Pedersen, E.; Schäffer, C. E. *Acta Chem. Scand.* **1970**, *24*, 247.

0020-1669/87/1326-2493$01.50/0

Table I. $\langle\tau\rangle^a$ (μs) for *cis*-$Cr(phen)_2F_2^+$ at 77 K

	λ, nm							
solvent	720	730	740	750	760–770	790–800	810–820	840–850
DMF/H_2O: X_{H_2O}								
0				827 (1.23)[b]	570 (1.37)	350 (1.49)		270 (1.45)
0.04			1000 (1.33)	790 (1.27)	650 (1.33)	400 (1.47)	320 (1.49)	
0.32			980 (1.30)		620 (1.47)	390 (1.64)	320 (1.61)	300 (1.67)
0.65		1233 (1.15)	980 (1.18)			420 (1.53)		
0.80	1625 (1.08)	1250 (1.16)			820 (1.45)			
EGW	1486 (1.09)	1343 (1.09)						
2-ME		1210 (1.12)			647 (1.54)		396 (1.79)	380 (2.0)

[a] $\langle\tau\rangle$ from single exponential fit for $I(0)$–$0.10I(0)$. [b] Values in parentheses are defined as $\bar{\tau}_f/\bar{\tau}_i$ (see Experimental Section).

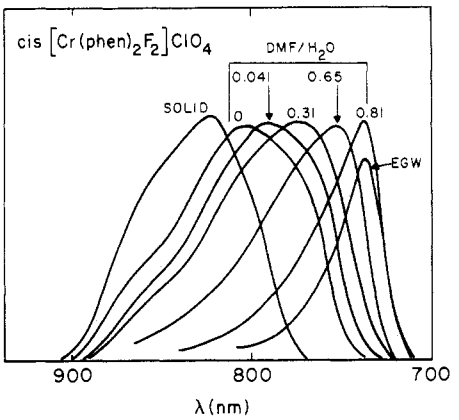

Figure 1. 77 K emission spectra at 25-μs delay of *cis*-$[Cr(phen)_2F_2](ClO_4)$. X_{H_2O} is designated for DMF/H_2O solutions.

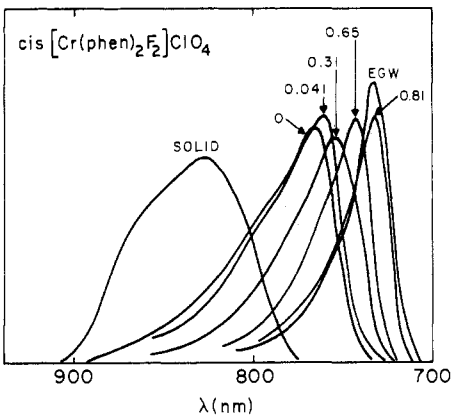

Figure 2. 77 K emission spectra at 1200-μs delay of *cis*-$[Cr(phen)_2F_2](ClO_4)$ as the solid and in EGW and DMF/H_2O solutions.

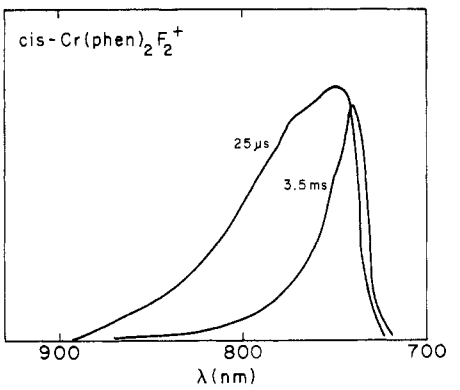

Figure 3. 77 K emission spectra of *cis*-$Cr(phen)_2F_2^+$ in 2-ME as a function of delay time.

***trans*-$Cr(py)_4F_2^+$.** The emission spectrum is the broad $^2E^Q \rightarrow {}^4A_2$ band in all solvents (Figure 4 and ref 2b), and there is very little change in the time-resolved spectra with delay time in EGW and DMF. The steep intensity decrease beyond 900 nm is due to the diminution of the detector sensitivity. The spectral widths in DMF and EGW are comparable when the detector is a photomultiplier with an S-1 response. The decays in EGW and DMF are fairly exponential with little wavelength dependence. The lifetime is 180 μs in EGW and 90 μs in DMF. The decays are less exponential in 2-ME with τ = 200 μs at 780 nm and 150 μs at 840 nm.

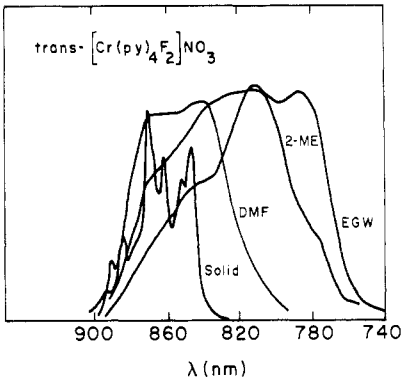

Figure 4. 77 K emission spectra of *trans*-$[Cr(py)_4F_2](NO_3)$ at 50-μs delay in different environments.

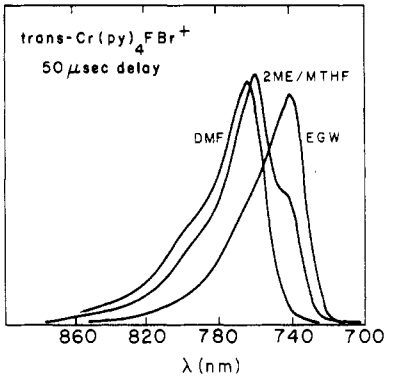

Figure 5. 77 K emission spectra of *trans*-$[Cr(py)_4FBr](ClO_4)$ at 50-μs delay in different environments.

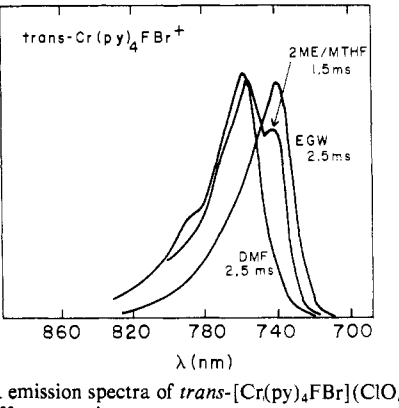

Figure 6. 77 K emission spectra of *trans*-$[Cr(py)_4FBr](ClO_4)$ at 1.5–2.5 ms delay in different environments.

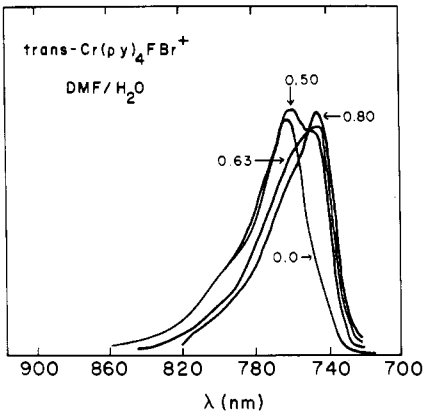

Figure 7. 77 K emission spectra of *trans*-$Cr(py)_4FBr^+$ at 25-μs delay in DMF/H_2O solutions at the indicated compositions (X_{H_2O}).

Table II. $\langle\tau\rangle^a$ (μs) for *trans*-$Cr(py)_4FBr^+$ at 77 K

	λ, nm			
solvent	743 ± 2	761 ± 2	780 ± 2	800 ± 1
EGW	710 (1.04)[b]		670 (1.09)	
DMF/H_2O: X_{H_2O}				
0		560 (1.27)		570 (1.35)
0.31		650 (1.08)		660 (1.18)
0.50	827 (1.05)	740 (1.05)		710 (1.18)
0.63	820 (1.06)		730 (1.14)	
0.80	767 (1.03)		710 (1.06)	
2-ME/MTHF (1:2.5 v/v)	837 (1.03)	639 (1.09)	641 (1.04)	

[a] $\langle\tau\rangle$ from single exponential fit for $I(0)$–$0.1I(0)$. [b] Values in parentheses are defined as $\bar{\tau}_f/\bar{\tau}_i$ (see Experimental Section).

The emission spectrum of solid *trans*-$[Cr(py)_4F_2](NO_3)$ is much more structured than the spectrum of solid *cis*-$[Cr(phen)_2F_2](ClO_4)$.

***trans*-$Cr(py)_4FBr^+$.** The emission is narrow in both DMF and EGW, but the spectral position is solvent dependent with maxima at 763 nm in DMF and at 743 nm in EGW (Figures 5 and 6). The behaviors of *trans*-$Cr(py)_4FCl^+$ and *trans*-$Cr(py)_4FBr^+$ are very similar. The emission spectra in DMF and DMF/H_2O (X_{H_2O} = 0.31) are identical (Figure 7). At higher water levels the shoulder at 745 nm is intensified progressively until at X_{H_2O} = 0.80 the 763-nm peak has disappeared and the emission is nearly coincident with the emission in EGW. The decays at 745 nm are exponential, but the lifetime is a function of X_{H_2O} (Table II).

In a mixed 2ME–MTHF glass two peaks are observed. One of these is coincident with the EGW peak while the other peak position is identical with that in DMF. The relative peak heights vary with the delay time in accord with the lifetime differences for emission monitored at the peaks (Figures 5 and 6).

***cis*-$Cr(bpy)_2Cl_2^+$.** The emission spectra are nearly identical in EGW, DMF, and DMF/H_2O glasses as well as in the solid. There is a slight change in the emission spectrum with delay time in both 2-ME and EGW (Figure 8). The emission spectra in 2-ME and 2-ME/MTHF are identical. The 10-nm difference between the maxima in 2-ME and EGW is somewhat larger than that observed in other cases of $^2E \rightarrow {}^4A_2$ emission.[2b] The solid *cis*-$[Cr(bpy)_2Cl_2]Cl\cdot 2H_2O$ spectrum is sharper than that of the cation in any of the glassy matrices and intermediate in position between the emissions in 2-ME and EGW. In dry DMF, either microcrystalline or glassy, *cis*-$Cr(bpy)_2Cl_2^+$ decomposes in the laser beam, but neither the emission spectrum nor the decay time changes with irradiation time. No decomposition was detectable in EGW or 2-ME. The decay is quite exponential in EGW with τ = 1060 μs.

$Cr(bpy)_3^{3+}$. The narrow solvent-independent emission spectrum of this complex is clearly due to $^2E \rightarrow {}^4A_2$ (Figure 8). Except in DMF, the 77 K lifetime of 5.2 ms is also solvent invariant. In DMF, $Cr(bpy)_3^{3+}$ decomposes so rapidly in the light beam that it was difficult to obtain a precise lifetime, but the spectrum does not change with irradiation time. Nonetheless, the recorded lifetime of 3.2 ms indicates a significant photoreaction that competes with excited state decay.

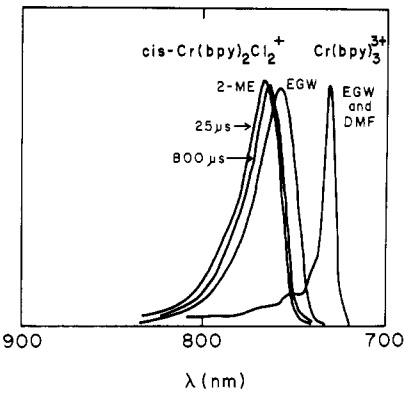

Figure 8. 77 K emission spectra of *cis*-$Cr(bpy)_2Cl_2^+$ and $Cr(bpy)_3^{3+}$ in different solvents.

Discussion

Although the designations of the $^2E \rightarrow {}^4A_2$ transitions as narrow and the $^2E^Q \rightarrow {}^4A_2$ transitions as broad are based on admittedly imprecise visual criteria, the low-temperature spectra of Cr(III) complexes in crystals provide a rationale for the classification scheme. When ^2E is the lowest excited level, the crystal spectra are of two types. In complexes with a centrosymmetric skeleton, e.g., $Cr(NH_3)_6^{3+}$,[6] *trans*-$Cr(en)_2Cl_2^+$,[7] and $Cr(CN)_6^{3-}$,[8] the *0–0* band is not the most intense feature, but a large fraction of the emission intensity falls within a few hundred reciprocal centimeters of the origin. In glassy media much of the vibronic structure is unresolved, but a similar intensity distribution prevails.[2b,9] In noncentrosymmetric complexes, the *0–0* band is dominant in the crystal spectra,[3,10] and the corresponding spectra in glasses usually consist of very narrow bands with weak shoulders.[2b,9] The absence of intense vibronic progressions indicates that the geometries of the ground and excited states are nearly identical. Whether or not there is a center of symmetry, the spectral positions in this group are nearly invariant to environment in either crystalline or glassy media.[1,2,11]

The low-temperature crystal emission spectra of *trans*-$Cr(py)_4F_2^+$,[4] *trans*-$Cr(en)_2F_2^+$,[4] and $Cr(NH_3)_5(OH)^{2+}$[12] stand in sharp contrast to the $^2E \rightarrow {}^4A_2$ spectra and are distinguished by a series of vibronic bands with similar intensities spanning a range in excess of 1000 cm^{-1}. The emission in these complexes has been assigned as $^2E^Q \rightarrow A_2$ and the spectral breadth attributed to a geometry change accompanying excitation. The Cr–F bonds in *trans*-$Cr(py)_4F_2^+$ are 0.01 nm shorter in the excited state than in the ground state.[4] The vibronic structure is obscured in low-temperature glasses, and the emission envelope is broad and relatively featureless. The width of the *trans*-$Cr(py)_4F_2^+$ emission in a glass is consistent with the solid-state spectrum. The environmental dependence of the $^2E^Q \rightarrow {}^4A_2$ spectral positions has been documented.[2b]

The basic questions to be addressed in this work are the following: How are the ^2E and $^2E^Q$ levels affected by the micro-

(6) Flint, C. D.; Greenough, P. *J. Chem. Soc., Faraday Trans. 2* **1972**, *68*, 897.
(7) Flint, C. D.; Mathews, A. P. *J. Chem. Soc., Faraday Trans. 2* **1980**, *76*, 1381.
(8) Flint, C. D.; Greenough, P. *J. Chem. Soc., Faraday Trans. 2* **1974**, *70*, 815.
(9) Forster, L. S.; Fucaloro, A. F.; Rund, J. V. *J. Phys. Chem.* **1984**, *88*, 5012.
(10) Fields, R. A.; Haindl, E.; Winscom, C. W.; Khan, Z. H.; Plato, M.; Moebius, K. J. *J. Chem. Phys.* **1984**, *80*, 3082.
(11) Flint, C. D.; Greenough, P.; Mathews, A. P. *J. Chem. Soc., Faraday Trans. 2* **1973**, *69*, 23.
(12) DeCurtins, S.; Güdel, H. U.; Neuenschwander, K. *Inorg. Chem.* **1977**, *16*, 796.

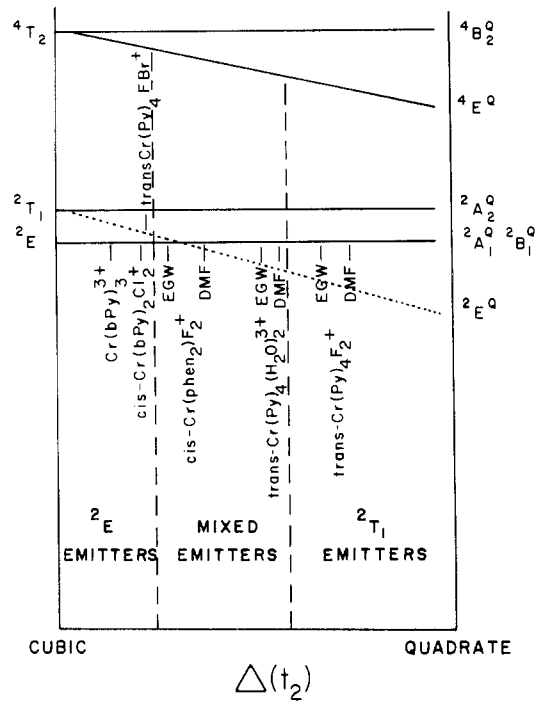

Figure 9. Energy levels (schematic) of d^3 complexes in quadrate fields. The approximate positions of ^2E and $^2E^Q$ are indicated for each complex.

environment in different solvents, and how does a change in these levels influence the emission characteristics? Ultimately, it is desirable to determine the structure of the multiple solvates and the manner in which the solute–solvent interactions influence the spectra and excited-state decay rates.

In the simplified picture that forms the basis of our analysis, the emission characteristics at 77 K depend on the relative positions of ^2E and $^2E^Q$ (Figure 9).[2b] The angular overlap model, which has been applied to the interpretation of the $^4T_2$ and $^4T_1$ splittings in *trans*-$Cr(py)_4XY$ complexes,[13] predicts that the magnitude of the $^2T_1$ splitting into $^2E^Q$ and $^2A_2^Q$ is a function of a single parameter, $\Delta(t_2)$, which is a measure of the difference in π-donation propensity between the axial and equatorial ligands. The quantitative applicability of the angular overlap model will be discussed below.

When ^2E is much lower than $^2E^Q$, e.g., in $Cr(bpy)_3^{3+}$ (Figure 8), a narrow solvent-insensitive $^2E \rightarrow {}^4A_2$ band is observed. These complexes are termed ^2E emitters. If $^2E^Q$ is sufficiently below ^2E as in *trans*-$Cr(bpy)_4F_2^+$, the emission is the broad solvent dependent $^2E^Q \rightarrow {}^4A_2$ band and complexes in this group are designated as $^2T_1$ emitters. But what of the intermediate cases where the ^2E–$^2E^Q$ separation is small? In cubic symmetry, there is no vibronic mixing between $^2T_1$ and ^2E since both states belong to the same half-filled configuration, t_2^3.[14] However, tetragonal distortions could lead to mixing between ^2E and $^2E^Q$ and the vibronic interactions would increase as the separation between the two levels is reduced. Under these conditions, the emission is intermediate in breadth between the "pure" ^2E and $^2T_1$ emissions. We have called this mixed emission.[2b]

When ^2E and $^2E^Q$ are close together, the spectrum will be very sensitive to small changes in the energy separation. This sensitivity could be due to variations in the vibronic mixing, but if both levels are thermally populated the emission will reflect emission from ^2E and $^2E^Q$. The relation between the individual ligands and the $^2T_1$ splitting will be treated below. It has been argued that *cis*-$Cr(NH_3)_4(OH)_2^+$ is an example of a complex in which the separation between ^2E and $^2E^Q$ is small.[2b] The solvent-dependent spectral behavior of *cis*-$Cr(phen)_2F_2^+$ indicates that in this species the separation of these two levels is also minimal.

Multiple Solvates in Low-Temperature Glasses. A distribution of fixed solvent environments prevails in any glassy matrix where the solvent rigidity inhibits molecular motion. The effect of microenvironmental heterogeneity on the emission is small when ^2E is much below $^2E^Q$ because the $^2E \rightarrow {}^4A_2$ emission exhibited by most Cr(III) complexes is nearly solvent invariant.[2a] On the other hand, the $^2E^Q \rightarrow {}^4A_2$ spectral position and lifetime vary considerably with solvent. The observation of a spectral shift has been advanced as a criterion for assigning the emission as $^2T_1$.[2b] The near exponentiality of the *trans*-$Cr(py)_4F_2^+$ $^2E^Q$ decays in DMF and EGW indicates that most of the emission from this complex in any medium is due to a single solvate or to a small group of solvates with very similar decay rates.

In *cis*-$Cr(phen)_2F_2^+$ different solvates have appreciably different spectra and decay times. Nonexponential decay is the result. This great sensitivity to environment makes *cis*-$Cr(phen)_2F_2^+$ a good probe for environmental heterogeneity. The 25-μs delay spectra of *cis*-$Cr(phen)_2F_2^+$ (Figures 1 and 3) reflect contributions from all solvates. The full range of DMF/H_2O spectra cannot be explained as a superposition of emission from two solvates, one hydrogen bonded and the other nonhydrogen bonded. As the water level is increased from X_{H_2O} = 0.0–0.31, the progressive blue shift is not accompanied by an increase in the band breadth, suggesting a cooperative effect in which the average environment is the determining factor. The marked shift between X_{H_2O} = 0 and 0.041 demonstrates the effect of small amounts of water on the DMF glass structure. At X_{H_2O} = 0.81 the environment approximates that in the hydroxylic EGW solvent. Only a subset of the *cis*-$Cr(phen)F_2^+$ solvate distribution is sampled in a long delay spectrum. Even in dry DMF, where hydrogen bonding is absent, several solvates with differing decay and spectral properties coexist (Figures 1 and 2). Smaller decay rates are associated with larger transition energies. The more than threefold difference in decay rates for emission monitored at 750 and >800 nm in dry DMF is at least partially due to the energy gap difference,[15] but the solvate structure may also play a role.

Since the short delay spectrum of *cis*-$Cr(phen)_2F_2^+$ in pure DMF is composed of contributions from a solvate distribution, it is difficult to assess the spectral breadth of the emission band from an individual solvate, but the Figure 1 spectra indicate that the dominant species have broad spectra until the water content becomes very high. This conclusion is reinforced by the long delay spectra (Figure 2), which are narrower than the short delay counterparts but still broader than the typical $^2E \rightarrow {}^4A_2$ emission as well as the emission of *cis*-$Cr(phen)_2F_2^+$ in hydroxylic solvents.

The change in the $Cr(NH_3)_4(OH)_2^+$ spectrum from broad in DMF to narrow in EGW was ascribed to an inversion of the ^2E–$^2E^Q$ order in the two solvents.[2b] Solvent-induced level inversion also prevails in *cis*-$Cr(phen)_2F_2^+$. Level inversion indicates that the $\Delta(t_2)$ values in EGW and DMF bracket the ^2E–$^2E^Q$ intersection (Figure 9). If the broad emission in *cis*-[$Cr(phen)_2F_2$](ClO_4) is assigned as $^2E^Q \rightarrow {}^4A_2$ and the narrow emission of this complex in EGW is $^2E \rightarrow {}^4A_2$, the spectra in DMF/H_2O show that the $^2E^Q$ energy is increased with water content in the mixed solent. At X_{H_2O} = 0.81 the DMF/H_2O emission is somewhat broader than the $^2E \rightarrow {}^4A_2$ spectrum in EGW, where X_{H_2O} is 0.61, but the positions are nearly identical. Although there are some differences in shape, the positions of the *trans*-$Cr(py)_4F_2^+$ spectra in EGW and DMF/H_2O (X_{H_2O} = 0.80) are also the same.[2b]

In contrast to the multiple solvate analysis that is required for glassy solutions of *cis*-$Cr(phen)_2F_2^+$, a two-species picture is adequate for the interpretation of the *trans*-$Cr(py)_4FBr^+$ spectra. The spectrum of the latter complex exhibits little delay dependence in either DMF or EGW. The solvate distribution is narrow in each of these two solvents, but the solvent spectral shift is larger than is usually observed for a $^2E \rightarrow {}^4A_2$ transition. Moreover, the bands are somewhat broader than a typical $^2E \rightarrow {}^4A_2$ spectrum. There is no evidence for ^2E–$^2E^Q$ level inversion in *trans*-$Cr(py)_4FBr^+$ when the solvent is changed from DMF to EGW. Instead, the emitting level energy merely changes with solvent.

(13) Glerup, J.; Mønsted, O.; Schäffer, C. E. *Inorg. Chem.* **1976**, *15*, 1399.
(14) Ceulemans, A.; Beyens, D.; Vanquickenbourne, L. G. *J. Am. Chem. Soc.* **1982**, *104*, 2988.
(15) Forster, L. S.; Mønsted, O. *J. Phys. Chem.* **1986**, *90*, 5131.

We suggest that the emitting level in both solvents is primarily ^2E but with an admixture of $^2E^Q$ due to vibronic coupling. This leads to some broadening and a small solvent dependence. The two-solvate model is supported by the emission in 2-ME/MTHF, where the spectrum at each delay can be viewed as a superposition of the DMF and EGW spectra. The spectra of this complex in DMF/H_2O solutions appear to be composite, consisting of emission from two species in proportions that vary with the water content. Since the spectra are not very different in DMF and EGW, no effect of cooperativity in DMF/H_2O solutions is evident. The decays of the 743- and 763-nm peaks, although somewhat different, are quite exponential (Table II), indicating separate but nearly homogeneous emitting populations in each of the spectral regions.

How Does Environment Alter Transition Energies? As described above, the variation in shape and position can be reasonably well rationalized in terms of a model in which the ^2E and $^2E^Q$ energies are the principal determinants. These energies, in turn, are influenced by intramolecular and intermolecular factors.

The dependence of spectral energies upon solvent has received great attention,[16] but the correlation of spectral shifts with bulk solvent properties is tenuous.[17] Solute–solvent interactions responsible for spectral shifts include general interactions, e.g., ion–dipole and dipole–dipole, and specific interactions, e.g., hydrogen bonding. Inhibition of solvent motions often has a profound effect on emission spectra, and blue shifts can arise from restriction in solvent rotations when dipolar interactions differ in the initial and final (Franck–Condon) states.[18]

All of the solvents employed in this work are polar. Disorder is frozen-in when the glass is formed, and a distribution of solvent orientations and solute–solvent separations prevails. Intermolecular interactions will restrict the range of solvates, and strong hydrogen bonding might result in a single dominant species, as in EGW solutions of *trans*-$Cr(py)_4F_2^+$.

Intermolecular interactions can also alter the intramolecular charge distributions, and the $^2T_1$ splittings would then be changed. The $^2T_1$ splitting is sensitive to the π-donation by F^-. The π-donation is reduced by hydrogen bonding.[19] Comparison of the EGW and DMF/H_2O spectra of *trans*-$Cr(py)_4FBr^+$ suggests that the 743-nm peak is due to hydrogen-bonded species while the 763-nm peak corresponds to the emission of non-hydrogen–bonded complexes. Although disruption of hydrogen bonding between water and the complex may influence the spectral shift in DMF/H_2O solutions of *cis*-$Cr(phen)_2F_2^+$, the cooperativity hypothesis requires that solvent–solvent interactions are important. An NMR study of DMF and H_2O rotational correlation times in mixed solvents has demonstrated that hydrogen bonding between water molecules is enhanced in the presence of DMF.[20] The rotational correlation times pass through maxima at X_{H_2O} = 0.25–0.30. The 25-μs delay spectrum of *cis*-$Cr(phen)_2F_2^+$ in 2-ME is significantly broader than that in EGW (Figures 1 and 3). The environment provided by the hydroxylic 2-ME is close to that in DMF/H_2O with X_{H_2O} = 0.65.

$Cr(bpy)_3^{3+}$ and *trans*-$Cr(py)_4F_2^+$ are nonpolar ions while the cis species and *trans*-$Cr(py)_4FBr^+$ are dipolar ions. Dipole–dipole interactions cannot be invoked to explain the solvent dependence of the $^2E^Q$ energy in the nonpolar ions. An alternative approach has been suggested in which interactions between solvent dipoles and solute monopoles are involved.[21] In Cr(III) complexes these monopoles would be ligand centered and the magnitude of a monopole–dipole interaction depends upon the distance between the ligand and the nearby solvent dipole. In the $^2E \rightarrow {}^4A_2$ transition there is no geometry change and both levels would be affected equally by alteration of the environment. However, there is a geometry change in the $^2E^Q \rightarrow {}^4A_2$ transition, and the transition energy would then be sensitive to the size of the solvent cavity in which the complex is embedded. The cavity size not only affects the $^2E^Q \rightarrow {}^4A_2$ transition energy by mediating the electrostatic interactions but also by inducing differential changes in the shapes of the potential surfaces in the two states. This point will be discussed in more detail in connection with solvent mobility changes.[22] The effect of X_{H_2O} on the *cis*-$Cr(phen)_2F_2^+$ spectra in DMF/H_2O glasses is due to the superposition of two factors, hydrogen bonding and solvent cavity size. It is difficult to separate the contributions from these two factors since the ligands that lead to the largest $^2T_1$ splittings, F^- and OH^-, will also hydrogen bond to hydroxylic solvents.

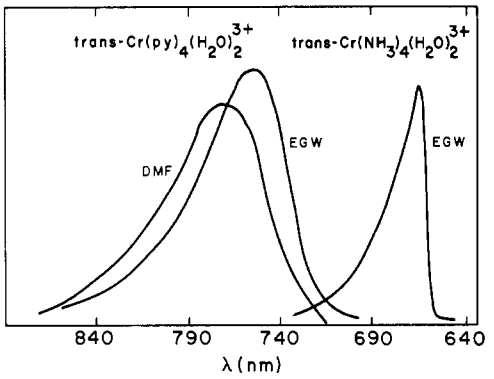

Figure 10. 77 K emission spectra of *trans*-$Cr(py)_4(H_2O)_2^{3+}$ and *trans*-$Cr(NH_3)_4(H_2O)_2^{3+}$.

Angular Overlap Model Parameters for Pyridine. In the angular overlap model the $^2T_1$ splitting of a *trans*-CrN_4X_2 complex depends quadratically upon the parameter

$$\Delta(t_2) = -\tfrac{1}{2}(\Delta'_{\pi X} - \Delta'_{\pi N}) \quad (1)$$

where $\Delta'_{\pi X}$ and $\Delta'_{\pi N}$ are the π-donation parameters of the axial X and equatorial N ligands, respectively.[13] If the axial ligands are different, holohedrized symmetry is assumed whereby each π-donation parameter is an average of the parameters for the ligands on a given axis

$$\Delta'_{\pi XY} = \tfrac{1}{2}(\Delta'_{\pi X} + \Delta'_{\pi Y}) \quad (2)$$

For *trans*-CrN_4XY complexes

$$\Delta(t_2) = -\tfrac{1}{2}(\Delta'_{\pi XY} - \Delta'_{\pi N}) \quad (3)$$

Application of holohedrized symmetry to *cis*-CrN_4X_2 complexes yields

$$\Delta(t_2) = \tfrac{1}{4}(\Delta'_{\pi X} - \Delta'_{\pi N}) \quad (4)$$

With NH_3 and ethylenediamine ligands, $\Delta'_{\pi N} = 0$. If $\Delta'_{\pi N}$ were negative for pyridine ligands, $\Delta(t_2)$ would be increased relative to amine coordination. In eq 3 and 4 the effect of twisting the pyridine ligands about the Cr–N bonds has been ignored. This neglect does not change the qualitative conclusions.

Two predictions follow from eq 3 and 4: (i) $\Delta(t_2)$ is twice as large in a *trans*-$Cr(NH_3)_4X_2$ complex than in the cis analogue; (ii) $\Delta(t_2)$ is the same in *cis*-$Cr(NH_3)_4X_2$ and $Cr(NH_3)_5X$. The emission in both *cis*-$Cr(NH_3)_4F_2^+$ and $Cr(NH_3)_5F^{2+}$ is $^2E \rightarrow {}^4A_2$ while the *trans*-$Cr(NH_3)_4F_2^+$ emission is $^2E^Q \rightarrow {}^4A_2$. ^2E and $^2E^Q$ are nearly coincident in *cis*-$Cr(NH_3)_4(OH)_2^+$ as evidenced by the solvent-induced state inversion,[2b] while $^2E^Q$ is definitely below ^2E in *trans*-$Cr(NH_3)_4(OH)_2^+$.[9] Both of these results are in accord with the predictions of the angular overlap model.

The absorption spectra of *trans*-$Cr(NH_3)_4XY$ and *trans*-$Cr(py)_4XY$ complexes have been used to extract $\Delta'_{\pi X}$ and $\Delta'_{\pi py}$ by assuming $\Delta'_{\pi NH_3} = 0$. A negative value for $\Delta'_{\pi py} < 0$ was obtained,[13] a result that has been disputed.[23] Since the $^2T_1$ splitting is a monotonic function of $\Delta(t_2)$, $^2E^Q$ emission in a *trans*-$Cr(py)_4X_2$ complex for which the emission from the *trans*-CrN_4X_2 analogue is ^2E, would indicate $\Delta'_{\pi py} < 0$. A negative $\Delta'_{\pi py}$ is supported by

(16) Nicol, M. *Appl. Spectrosc. Rev.* **1974**, *8B*, 183.
(17) Brady, J. E.; Carr, P. W. *J. Phys. Chem.* **1985**, *89*, 5759.
(18) Gudgin-Templeton, E. F.; Ware, W. R. *J. Phys. Chem.* **1984**, *88*, 4626.
(19) Glover, S. G.; Kirk, A. D. *Inorg. Chim. Acta* **1982**, *137*, L1982.
(20) Weingarten, H.; Holz, M.; Hertz, H. G. *J. Solution Chem.* **1978**, *7*, 689.
(21) Macgregor, R. B., Jr.; Weber, G. *Ann. N. Y. Acad. Sci.* **1981**, *366*, 140.
(22) Ghaith, A.; Forster, L. S.; Rund, J. V., to be submitted for publication.
(23) Gerloch, M.; Wooley, R. G. *Prog. Inorg. Chem.* **1984**, *31*, 371.

Table III

complex	solvent	emitting state	ΔE,[a] μm^{-1}	$10^4\tau^{-1}$, s^{-1}
trans-$Cr(py)_4F_2^+$	EGW	$^2E^Q$	1.238	0.50
	DMF	$^2E^Q$	1.19	1.1
trans-$Cr(py)_4Cl_2^+$	EGW	^2E	1.374	0.049
	DMF	^2E	1.387	0.044
trans-$Cr(py)_4Br_2^+$	EGW	^2E	1.391	0.042
	DMF	^2E	1.391	0.037
trans-$Cr(py)_4(H_2O)_2^{3+}$	EGW	$^2E^Q$	1.316	>1.0[b]
	DMF	$^2E^Q$	1.297	3.9
trans-$Cr(py)_4(D_2O)_2^{3+}$	EGW	$^2E^Q$	1.316	0.14–0.20
cis-$Cr(bpy)_2F_2^+$	EGW	^2E	1.359	0.100
	DMF	$^2E^Q$	1.25	0.25–0.40
cis-$Cr(phen)_2F_2^+$	EGW	^2E	1.370	0.111–0.063
	DMF	$^2E^Q$	1.282	0.104–0.35
cis-$Cr(bpy)_2Cl_2^+$	EGW	^2E	1.319	0.095
	DMF	^2E	1.317	0.080–0.10
cis-$Cr(bpy)_2(H_2O)_2^{3+}$	EGW	^2E	1.410	0.310
cis-$Cr(bpy)_2(D_2O)_2^{3+}$	EGW	^2E	1.410	0.045
cis-$Cr(bpy)_2(OH)_2^+$	EGW	$^2E^Q$	1.316	2.2–3.2
$Cr(bpy)_3^{3+}$	EGW	^2E	1.376	0.019
	DMF	^2E	1.367	0.031
trans-$Cr(py)_4FBr^+$	EGW	^2E	1.346	0.14
	DMF	^2E	1.311	0.18

[a] 0–0 band for ^2E emitters, band maximum for $^2E^Q$ emitters. [b] Very nonexponential.

the following observations: (1) the *trans*-$Cr(py)_4(H_2O)_2^{3+}$ emission is $^2E^Q \rightarrow {}^4A_2$ in EGW and DMF while *trans*-$Cr(NH_3)_4(H_2O)_2^{3+}$ is a ^2E emitter in both solvents (Figure 10); (2) *cis*-$Cr(phen)_2F_2^+$ and *cis*-$Cr(bpy)_2F_2^+$ are ^2E emitters in EGW but $^2T_1$ emitters in DMF, while the *cis*-$Cr(NH_3)_4F_2^+$ emission is $^2E \rightarrow {}^4A_2$ in DMF and EGW; (3) in EGW the *cis*-$Cr(bpy)_2(OH)_2^+$ emission is $^2E^Q \rightarrow {}^4A_2$ while the emission of *cis*-$Cr(NH_3)_4(OH)_2^+$ is $^2E \rightarrow {}^4A_2$ in the same solvent; (4) the spectrum of *cis*-$Cr(bpy)_2Cl_2^+$ broadens and shifts to longer wavelengths when the glass softens,[22] indicating that the ^2E–$^2E^Q$ vibronic mixing is enhanced when the $^2E^Q$ energy is reduced in the fluid. There are no analogous changes in the spectrum of *cis*-$Cr(NH_3)_4Cl_2^+$. However, the shapes of the *trans*-$Cr(py)_4FCl^+$ and *trans*-$Cr(en)_2FCl^+$ spectra in EGW are the same and do not indicate any change in the $^2E^Q$–^2E separation when pyridine ligands are replaced by 1,2-ethanediamine. Although not unambiguous, the weight of evidence favors a negative $\Delta'_{\pi py}$ for both pyridine and polypyridine ligands. It can be argued that $\Delta'_{\pi py}$ is not really negative but that pyridine ligation increases the $\Delta'_{\pi X}$ value of the axial ligands. Operationally, the two views cannot be distinguished, but the predictive power of the angular overlap model is not diminished by this uncertainty.

The relative ordering of $\Delta(t_2)$, as inferred from the spectral behavior, is indicated in Figure 9.

Nonradiative Rates and Structure. The 77 K values of τ^{-1} for a group of complexes with pyridine ligation are summarized in Table III. The radiatiave rate, k_r, is 100–300 s^{-1} in Cr(III) complexes. k_{nr}, the nonradiative rate, is very small in $Cr(bpy)_3^{3+}$ as it is in $Cr(CN)_6^{3-}$ and $Cr(NCS)_6^{3-}$. Good quenching ligands couple effective accepting modes such as the high frequency NH or OH vibrations to the metal-centered transition. Evidently the d-electron density does not interact with the high-frequency CH stretching modes in 2,2′-bipyridine, and this ligand is a poor quencher. $Cr(bpy)_3^{3+}$, *cis*-$Cr(bpy)_2Cl_2^+$, and *cis*-$Cr(bpy)_2(H_2O)_2^{3+}$ are ^2E emitters. Replacement of a single 2,2′-bipyridine group with two H_2O ligands does increase k_{nr} substantially, but the k_{nr} enhancement by the poor quencher, D_2O, is slight. To the extent that a decrease in the transition energy is accompanied by increased d-electron delocalization onto the pyridine ligands,[24] the energy gap effect will be larger in pyridine complexes than in those with amine ligands. This is due to increased coupling between the d electrons and the good accepting CH modes.[25] Consequently, the energy gap variation may be responsible for the twofold larger k_{nr} in *cis*-$Cr(bpy)_2Cl_2^+$ compared to that in *trans*-$Cr(py)_4Cl_2^+$ as well as the threefold difference between the *trans*-$Cr(py)_4FBr^+$ and *trans*-$Cr(py)_4Cl_2^+$ decay rates. The energy gap correlation is also evident in the decay rates of the *trans*-$Cr(py)_4(D_2O)_2^{3+}$–*trans*-$Cr(py)_4Cl_2^+$ and *cis*-$Cr(bpy)_2(D_2O)_2^{3+}$–*cis*-$Cr(bpy)_2Cl_2^+$ pairs. In the trans pair, the rate enhancement by D_2O is the larger and the energy gap the smaller, while the converse prevails in the cis pair. The near identity of the *trans*-$Cr(py)_4Br_2^+$ and *trans*-$Cr(py)_4Cl_2^+$ k_{nr} values is noteworthy and is in accord with the general lack of correlation between spin–orbit coupling constants and excited-state decay.[26]

Summary and Conclusions. Quadrate complexes can be categorized as $^2T_1$, ^2E, and mixed emitters. $Cr(bpy)_3^{3+}$ is a ^2E emitter, while *trans*-$Cr(py)_4F_2^+$ is a $^2T_1$ emitter. In ^2E emitters, ^2E is below $^2E^Q$ in all media, but the reverse ordering obtains in $^2T_1$ emitters. The near equality of the energies of the two levels in mixed emitters leads to marked solvent sensitivity, and in some cases, there is a state reversal between hydroxylic and nonhydroxylic solvents. *cis*-$Cr(phen)_2F_2^+$ is an example of this behavior. It is only in the mixed emitters that the effect of a solvate distribution is marked because small shifts in the $^2E^Q$ energy lead to large fractional differences in the ^2E–$^2E^Q$ separation. This in turn affects the vibronic mixing between the two levels.

The solvent effects on the spectrum of *trans*-$Cr(py)_4FBr^+$ indicate that specific hydrogen-bonded and non-hydrogen-bonded solvates are present in glassy solutions of this species. On the other hand, the *cis*-$Cr(phen)_2F_2^+$ spectra in DMF/H_2O solutions can only be interpreted in terms of distributions with multiple solvates whose character varies continuously with the solvent composition.

If $^2E^Q$ is not too far above ^2E in a $Cr(NH_3)_4X_2$ complex, changing amine coordination to pyridine coordination will serve to alter the emission spectrum either by level inversion or increased vibronic mixing.

Acknowledgment. We are grateful to J. Glerup and J. Josephsen for providing several of the complexes.

Registry No. *trans*-$Cr(py)_4F_2^+$, 47514-84-1; *trans*-$Cr(py)_4Cl_2^+$, 51266-53-6; *trans*-$Cr(py)_4Br_2^+$, 51266-52-5; *trans*-$Cr(py)_4(H_2O)_2^{3+}$, 51266-59-2; *trans*-$Cr(py)_4(D_2O)_2^{3+}$, 108711-58-6; *cis*-$Cr(bpy)_2F_2^+$, 47513-99-5; *cis*-$Cr(phen)_2F_2^+$, 26154-72-3; *cis*-$Cr(bpy)_2Cl_2^+$, 27803-22-1; *cis*-$Cr(bpy)_2(H_2O)_2^{3+}$, 36513-26-5; *cis*-$Cr(bpy)_2(D_2O)_2^{3+}$, 108711-59-7; *cis*-$Cr(bpy)_2(OH)_2^+$, 108812-97-1; $Cr(bpy)_3^{3+}$, 15276-15-0; *trans*-$Cr(py)_4FBr^+$, 51266-54-7.

(24) DeArmond, K.; Forster, L. S. *Spectrochim. Acta* **1963**, *19*, 1403.
(25) Robbins, D. J.; Thomson, A. J. *Mol. Phys.* **1973**, *25*, 1103.
(26) Forster, L. S.; Rund, J. V.; Fucaloro, A. F.; Lin, S. H. *J. Phys. Chem.* **1984**, *88*, 5020.